



HAL
open science

Photoabsorption windows for Na and Na²⁺

Xiao-Ying Han, Xiang Gao, Jia-Ming Li, Lan Voky, Nicole Feautrier

► **To cite this version:**

Xiao-Ying Han, Xiang Gao, Jia-Ming Li, Lan Voky, Nicole Feautrier. Photoabsorption windows for Na and Na²⁺. *Physical Review A*, 2006, 74, pp.62710. 10.1103/PhysRevA.74.062710 . hal-03742215

HAL Id: hal-03742215

<https://hal.science/hal-03742215v1>

Submitted on 9 Sep 2022

HAL is a multi-disciplinary open access archive for the deposit and dissemination of scientific research documents, whether they are published or not. The documents may come from teaching and research institutions in France or abroad, or from public or private research centers.

L'archive ouverte pluridisciplinaire **HAL**, est destinée au dépôt et à la diffusion de documents scientifiques de niveau recherche, publiés ou non, émanant des établissements d'enseignement et de recherche français ou étrangers, des laboratoires publics ou privés.

Photoabsorption windows for Na and Na₂⁺Xiao-Ying Han,^{1,*} Xiang Gao,² Jia-Ming Li,^{2,1,†} Lan Voky,^{3,‡} and Nicole Feautrier³¹*Key Laboratory of Atomic and Molecular Nanosciences of Education Ministry, Department of Physics, Tsinghua University, Beijing 100084, China*²*Department of Physics, Shanghai Jiao Tong University, Shanghai 200230, China*³*LERMA, UMR 8112 du CNRS, Observatoire de Paris, 92915 Meudon Cedex, France*

(Received 7 September 2006; published 18 December 2006)

There exist absorption windows (i.e., Cooper-minima) in the photoabsorption cross sections of some atomic systems because of the relative phase shifts between the initial and final state wave functions due to the atomic screening potentials in contrast to the Coulomb potentials. Such window positions are sensitive to the accuracy of the initial and final state wave functions. Using our modified Breit-Pauli R -matrix code, the photoionization cross sections of ground Na are calculated. Our calculated cross sections and minimum position in the low photoelectron energy range (<9 eV) are in excellent agreement with the experimental results. In the high energy range (>9 eV), there is an abnormal bump in the experimental measurements, which is a long-standing experimental puzzle. It is interesting to note that there is also an absorption window in the photoabsorption (i.e., photodissociation) cross sections of Na₂⁺. Such an absorption window provides an answer to the puzzle.

DOI: [10.1103/PhysRevA.74.062710](https://doi.org/10.1103/PhysRevA.74.062710)

PACS number(s): 32.80.-t, 31.25.-v, 32.70.Fw, 33.80.-b

I. INTRODUCTION

Photoexcitation and photoionization processes of atoms and molecules play important roles in laser physics, radiation physics, plasma physics, atmospheric physics, and astrophysics. The photoabsorption (including the photoexcitation and photoionization) cross sections are the indispensable physical parameters in the relative fields. The photoabsorption cross sections are directly proportional to the square of the dipole transition matrix elements. For particular initial states of some atomic systems, the dipole matrix elements may change sign when smoothly varying with the excitation energies because of the relative phase shifts between the initial and final state wave functions due to the atomic screening potentials in contrast to the Coulomb potentials [1–4]. Therefore there exist absorption windows (i.e., atomic Cooper-minima) in the photoabsorption cross sections at the energy where the transition matrix elements are zero. The absorption window positions are sensitive to the accuracy of the initial and final state wave functions. For Na, since the dipole transition matrix elements of $3s \rightarrow \epsilon p$ transitions change sign from “–” to “+” with increasing excitation energies due to the atomic screening potentials, there is an absorption window in the photoionization cross sections above threshold [1–8]. Using our modified Breit-Pauli R -matrix code the photoionization cross sections of ground Na are calculated. In our calculations, because of taking into account the relativistic effects (mainly the spin-orbit interactions), the matrix elements of two final channels $\epsilon p_{1/2}$ and $\epsilon p_{3/2}$ are zero at different energies. This splitting results in the nonzero total cross sections at the minimum position. Our calculated cross sections (especially the velocity form results) in the low photoelectron energy range (<9 eV) agree well with the experi-

mental results [9]. In the high energy range (>9 eV), there is an abnormal bump in the experimental results, which has been a long-standing experimental puzzle since 1967 [5–9]. It is interesting to note that there is also an absorption window (i.e., molecular Cooper-minimum) in the photoabsorption (i.e., photodissociation) cross sections of Na₂⁺. Such absorption window provides an answer for the experimental puzzle, i.e., the absorption window guarantees that the existence of Na₂⁺ does not affect the measured Na cross sections at low energies; the photodissociation cross sections above the molecular absorption window result in the abnormal bump in the experimental measurements.

II. THEORETICAL METHODS AND RESULTS

The detailed descriptions of the R -matrix method have been presented in the previous works [10–17]. Only a brief outline will be given here. This method begins by partitioning the subconfiguration space of the excited electron into two regions by a sphere of radius a centered on the nucleus; in this work $a=29.2$ a.u. In the external region $r > a$, where r is the distance of the excited electron relative to the centroid of the target, the exchange interactions between the excited electron and the target electrons are negligible. The excited electron mainly “feels” Coulomb potential as well as the long-range static polarization potential. Within the reaction zone $r \leq a$, the interactions between the excited electron and the target electrons involve electron exchange and correlation interactions. It is a many-electron problem, which is solved variationally as a whole to obtain the logarithmic derivative boundary matrix $\mathcal{R}(E)$. Therefore within the reaction zone the electron correlations for the $(N+1)$ -electron system including the target Na⁺ and an excited electron are calculated adequately by the variational method [18]. In order to take into account the relativistic effects, our calculations are employed within the Breit-Pauli approximation by adding spin-orbit interaction operator, mass-correction operator, and Darwin operator to the usual nonrelativistic Hamiltonian

*Electronic address: hanxiaoying@tsinghua.org.cn

†Electronic address: lijm@sjtu.edu.cn

‡Electronic address: lan.voky@obspm.fr

[16,19,20]. Therefore the initial and final state wave functions can be calculated by taking into account the electron correlations and the relativistic effects adequately on equal footing. The wave functions Ψ for the $(N+1)$ -electron system of eigenenergy E within the reaction zone are expanded as

$$\Psi = \sum_k A_{Ek} \Psi_k. \quad (1)$$

Here Ψ_k are the energy-independent bases, which are expanded by the following way:

$$\Psi_k = \mathcal{A} \sum_{ij} a_{ijk} \Phi_i \frac{1}{r_{N+1}} u_{ij}(r_{N+1}) + \sum_j b_{jk} \phi_j. \quad (2)$$

Here \mathcal{A} is the antisymmetrization operator which accounts for the electron exchanges between the target electrons and the excited electron. u_{ij} are the continuum orbitals. ϕ_j are formed from the bound orbitals to ensure the completeness of the total wave functions and take account of the electron correlations within the reaction zone. The coefficients a_{ijk} and b_{jk} are obtained by diagonalizing the Breit-Pauli Hamiltonian matrix of the $(N+1)$ -electron system. Φ_i are the channel wave functions obtained by coupling the target wave functions with the angular momentum and spin of the excited electron. In this work, we adopt the same target orbital and configuration bases to those of the previous paper [21]. More specifically, the first important 111 target states in J^π representation are adopted, which arise from four kinds of configurations: $2p^6$, $2p^5nl$, $2p^4nl'n'l'$, $2p^3nl'n'l'n''l''$. Our calculated lowest 15 target state energy levels agree well with the experimental values [22] within 1%. Through these target states the monopole and higher multipole polarization effects with the exchange correlations between the target electrons and the excited electron can be considered. The wave functions with $J^\pi=(1/2)^e$ symmetry, involving the initial state wave function, are expanded by 202 channel wave functions; the wave functions with $(1/2)^o$ and $(3/2)^o$ symmetries are expanded by 202 and 345 channel wave functions, respectively. Our calculated lowest ionization energy of ground Na[$2p^63s$] converges to 0.3804 Ry, which agrees well with the experimental value 0.3777 Ry [22] by about 0.7%. The agreement manifests that not only the good convergence of Na⁺ and Na systems but also the good balance between the initial bound and final continuum states are obtained.

In the R -matrix method, using the dipole transition matrices, a generalized line strength for a transition from an initial bound state i of energy E_i to a final continuum state f of energy $E_f=E_i+\omega$ (in Rydbergs) in the length and velocity forms is defined [16]:

$$S_L(E_f, i) = \sum_{\tilde{L}_f} |(\tilde{L}_f E_f || D_L || i)|^2 \\ = \sum_{\tilde{L}_f} \left| \int_0^{R_0^L(\omega)} d\vec{r} \psi_f \vec{r}_n \psi_i + \int_{R_0^L(\omega)}^{R_{cut}^L} d\vec{r} \psi_f \vec{r}_n \psi_i \right|^2, \quad (3)$$

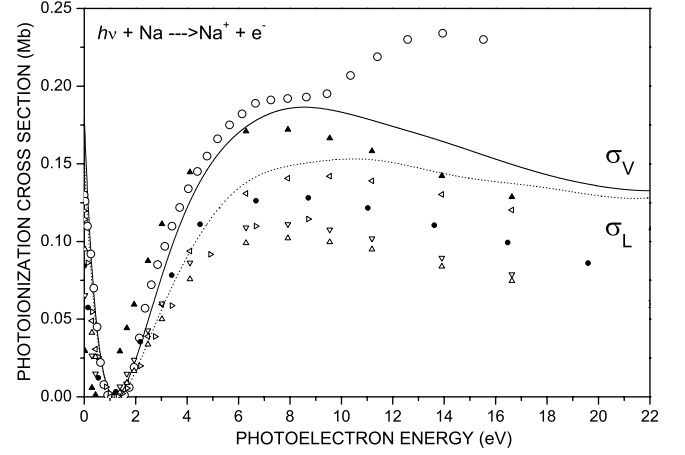


FIG. 1. (○): the experimental measurements of Ref. [9]; (—): the present Breit-Pauli R -matrix calculation results in the velocity form; (···): the present Breit-Pauli R -matrix calculation results in the length form; (◁): MCHF calculation results of Ref. [5] in the length form; (▲): the many-body calculation results of Ref. [6] in the length form; (△, ▽): the HF calculation results of Ref. [6] in the velocity and length forms, respectively; (●): calculation results of Ref. [7]; and (▷): calculation results of Ref. [8].

$$S_V(E_f, i) = 4\omega^{-2} \sum_{\tilde{L}_f} |(\tilde{L}_f E_f || D_V || i)|^2 \\ = \sum_{\tilde{L}_f} \left| \int_0^{R_0^V(\omega)} d\vec{r} \psi_f \frac{d\psi_i}{d\vec{r}_n} + \int_{R_0^V(\omega)}^{R_{cut}^V} d\vec{r} \psi_f \frac{d\psi_i}{d\vec{r}_n} \right|^2. \quad (4)$$

Here $D_L = \sum_n \vec{r}_n$ and $D_V = \sum_n \vec{\nabla}_n$, where the summation is over all the electrons. l_f and \tilde{L} are the angular momenta for the photoelectron and the residual ion, respectively. ω is the photon energy in Rydbergs. $R_0(\omega)$ is a turn point, by which the whole integrations for S are separated into two parts: in the inner region $r < R_0(\omega)$, the integration contributions are negative, in the outer region $r > R_0(\omega)$, the integration contributions are positive [2]. $R_0(\omega)$ decreases with increasing ω and $R_0^V(\omega) < R_0^L(\omega)$. Note that, here $R_0(\omega)$ is different from the R -matrix box radius a . R_{cut} is the integration limit. $R_{cut}^V < R_{cut}^L$, i.e., S_L is sensitive to the overlapping of the initial and final state wave functions at large distances; S_V is sensitive to the overlapping of the final state wave functions and the differential of the initial bound state wave functions at short distances. The photoionization cross section is usually calculated as

$$\sigma_{L(V)} = \frac{4}{3} \pi^2 a_0^2 \alpha \frac{\omega}{g} S_{L(V)}, \quad (5)$$

where g is the statistical weight of the initial bound state and S is calculated using the final state wave functions normalized per Rydberg. The constant in Eq. (5) is $\frac{4}{3} \pi^2 a_0^2 \alpha = 2.689$ Mb.

Figure 1 shows the photoionization cross sections of ground Na. Our calculation results (especially the velocity form results) agree well with the experimental measurements [9] in the low photoelectron energy range (< 9 eV). In the

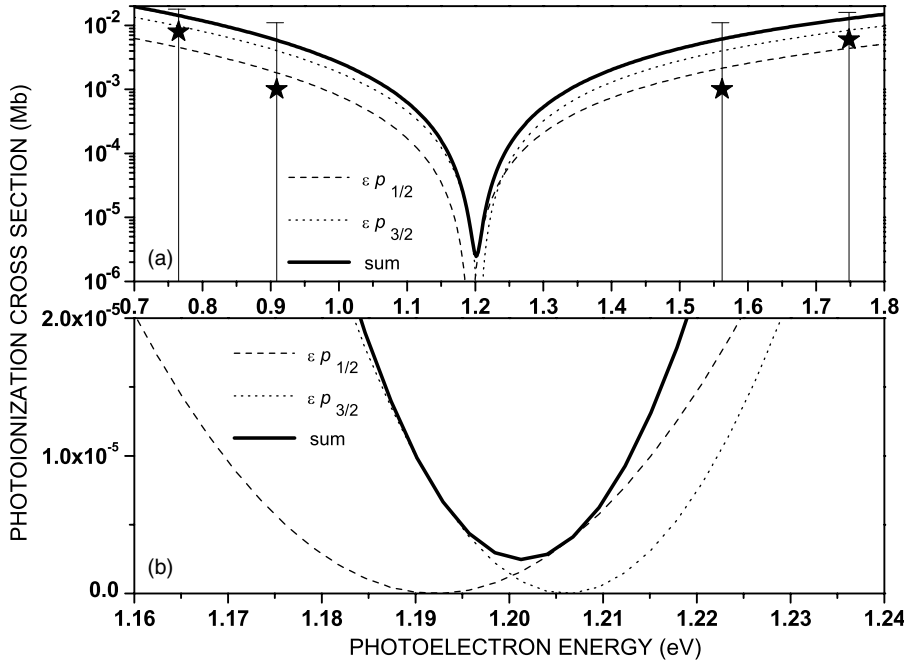


FIG. 2. The partial and total photoionization cross sections of ground Na near the Cooper-minimum positions. (★): the experimental measurements of Ref. [9] with 0.01 Mb error bar; (---) and (···): the partial cross sections of two final channels $\epsilon p_{1/2}$ and $\epsilon p_{3/2}$ in the velocity form; and (—): the total cross sections.

energy range below and at the minimum position (~ 1.2 eV), our calculated σ_V and σ_L agree with each other. In the energy range above the minimum position, our calculated σ_V are in better agreement with the experimental results than σ_L . However, at higher energies (>17 eV) σ_V and σ_L merge together again within 1%. Such an interesting feature can be understood as follows. At the minimum position, where the corresponding $R_0(\omega)$ is labeled as $R_0(\omega_0)$, for S_L and S_V the inner region negative contributions and the outer region positive contributions are canceled absolutely. At the energy above the minimum position, where $R_0^L(\omega) < R_0^L(\omega_0)$, σ_L is very sensitive to the small net value of the outer region positive contributions at large distances. However, for the energy normalized final channel wave functions, their small distance wave functions have the same feature, thus σ_V still have the same accuracy as those at the minimum position since the main integrations of σ_V are completed at small distances. Therefore it can be understood that in the energy range above the minimum position, σ_V are in better agreement with the experimental results than σ_L , which manifest that the small distance wave functions have sufficient accuracy. It is expected that with the improved large distance wave functions, σ_L will converge to σ_V in this energy range. At high energies (>17 eV), $R_0^L(\omega)$ becomes further smaller and the positive net value of the outer region contributions becomes larger. Furthermore, the percentage of the large distance wave-function contributions reduces. Therefore σ_L and σ_V merge together again. The excellent agreement between the theoretical and experimental results demonstrates that both the electron correlations and the relativistic effects are treated adequately on equal footing. As shown in Fig. 1, the other theoretical results ($\triangleleft, \triangle, \nabla, \bullet, \triangleright$) [5–8] have the accordant minimum positions with the experimental results, while their calculated cross sections above the minimum position are smaller than our calculation results. Although the many-body calculation results (\blacktriangle) [6] have good agreement be-

tween the length and velocity form results, their minimum position is lower than the experimental results. It is noted that in the high energy range (>9 eV), there is an abnormal bump in the experimental results higher than all the theoretical calculation results, which has been a long-standing experimental puzzle for several decades and will be discussed later.

Let us return to discuss the delicate feature of the cross sections at the minimum position. Although our calculated Cooper-minimum position agrees with the experimental results as shown in Fig. 1, our calculated total cross sections at the minimum position are very small ($\sim 10^{-6}$) but not zero as shown in Fig. 2. The nonzero minimum feature is due to the relativistic effects (mainly the spin-orbit interactions), which result in the dipole transition matrix elements of the two final channels $\epsilon p_{1/2}$ and $\epsilon p_{3/2}$ to be zero at different energies as shown in Fig. 2(b). This subtle splitting deserves further experimental studies since a precision measurement of the separated minimum positions will provide a “benchmark” experiment to test the theoretical method. Note that, at the separated zero minimum positions, using the polarized photons, the photoelectrons with the largest spin polarizations ($=1$) can be obtained [23].

III. DISCUSSIONS AND CONCLUSION

In the following, we will discuss the abnormal bump of the experimental results in Fig. 1. For illustrating clearly, the bumps are plotted in Fig. 3, which are obtained by subtracting our calculated σ_V from the experimental results. Reference [9] pointed out that there are mixed Na₂ molecules (within about 10%) in their measurements. The contributions of Na₂ have been corrected appropriately by Eq. (1) of Ref. [9]: $\ln[I_0(\lambda)/I(\lambda)] = C_a \sigma_a^{eff}(\lambda)L + C_m \sigma_m(\lambda)L$. Here, $I_0(\lambda)$ and $I(\lambda)$ are the incident and transmitted intensities, respectively. C_a and C_m are the concentrations of the atomic and molecu-

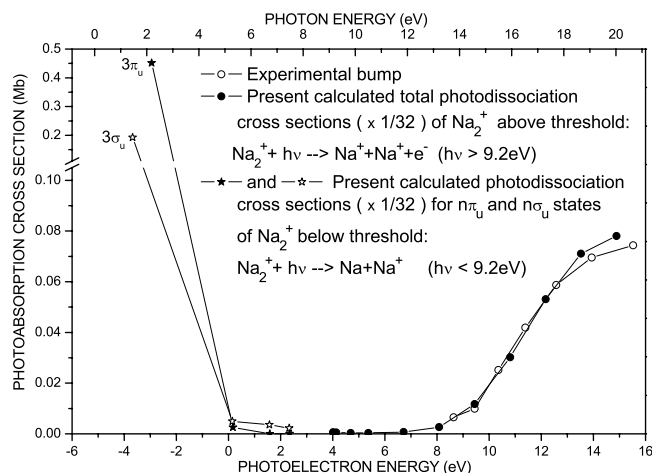


FIG. 3. The experimental bump (\circ) is obtained by subtracting our calculated σ_V from the experimental values [9]. Our calculated first ionization threshold of Na_2^+ is about 9.2 eV.

lar species. $\sigma_a^{eff}(\lambda)$ and $\sigma_m(\lambda)$ are the absorption cross sections of atomic and molecular species. L is the path length. Note that the energy level of the first excited state [$2p^53s$] of Na^+ is 32.8 eV relative to ground Na^+ [22], therefore the bump cannot result from the photoabsorption processes of Na^+ . Since the first ionization threshold (4.9 eV) of Na_2 [24] is smaller than the first ionization threshold (5.139 eV) of Na [22], there should exist some Na_2^+ in their experiment.

Thus $\sigma_a^{eff}(\lambda) = \sigma_a(\lambda) + \frac{C_i}{C_a} \sigma_i(\lambda)$, where the concentration C_i and cross section σ_i are for the ionic molecule Na_2^+ . To our knowledge the theoretical and experimental studies of Na_2^+ are scarce. Here, using the multiple-scattering self-consistent field (MSSCF) method [25–30], we calculated the photoabsorption (i.e., photodissociation) cross sections of Na_2^+ by evaluating the transition matrix elements. More specifically, the ground state configuration of Na_2^+ is $(\text{Na } 1s)^2(\text{Na } 1s)^2(\text{Na } 2s)^2(\text{Na } 2s)^2(\text{Na } 2p)^6(\text{Na } 2p)^6(4\sigma_g)^1$. Our calculated first ionization threshold of Na_2^+ is about 9.2 eV. According to the transition selection rules, the $4\sigma_g$ electron can be excited mainly into $n p \pi_u / \epsilon p \pi_u$ and $n p \sigma_u / \epsilon p \sigma_u$ channels. Our calculated eigenquantum defects of the two eigenchannels $p \pi_u$ and $p \sigma_u$ are plotted in Fig. 4. In the framework of the quantum defect theory (QDT) [31–34], all the molecular orbitals, involving the bound and adjacent continuum molecular orbitals, are treated in a unified manner. Using the channel wave functions, we calculated the corresponding oscillator strength densities, which are directly proportional to the cross sections. The cross sections are plotted in Fig. 3. In order to explain the experimental bump quantitatively, in Fig. 3, the photodissociation cross sections of Na_2^+ are multiplied by 1/32 (i.e., $C_i/C_a=1/32$). It can be found that the energy level positions of $3\pi_u$ and $3\sigma_u$ states are below zero, i.e., below the energy range of Na measurements, therefore the cross sections of $3\pi_u$ and $3\sigma_u$ states nearly do not affect the measurements of Na . Moreover, it is interesting to note that there is an absorption window (i.e., molecular Cooper-minimum) in the photodissociation cross sections of Na_2^+ in the energy range (0–9 eV), which guarantees that the existence of Na_2^+ does not affect

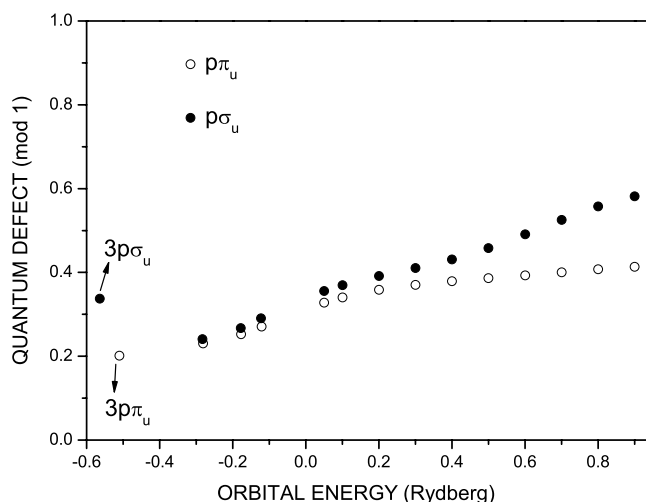


FIG. 4. Our calculated eigenquantum defects for eigenchannels $p \pi_u$ and $p \sigma_u$.

the measurements of Na in the low energy range. Note that, for the bound states (e.g., $3\pi_u$ and $3\sigma_u$), our calculated photodissociation cross sections are the integrated cross sections without any expansion. However, experimentally, the measured photodissociation cross sections have a vibrational distribution, which will be reported in detail elsewhere [35]. In the high energy range (>9 eV), our calculated photodissociation cross sections are in good agreement with experimental abnormal bump. Therefore the bump should result from the photodissociation processes of Na_2^+ . The concentration C_i/C_a of Na_2^+ is estimated to be about 3% (1/32), which is consistent with the experimental conditions that the concentration of Na_2 is within 10%.

In conclusion, we would like to make the following comments. Using our modified Breit-Pauli R -matrix code the photoionization cross sections of ground Na are calculated, which involve bound and continuum state wave functions. Because of considering the relativistic effects (mainly the spin-orbit interactions) our calculated total cross sections are not zero at the minimum position. As shown in Fig. 1, our calculated cross sections (especially the velocity form results) and minimum position in the low photoelectron energy range (<9 eV) are in good agreement with the experimental results [9]. In the high energy range (>9 eV), there is an abnormal bump in the experimental results. It is interesting to note that there is also an absorption window in the photodissociation cross sections of Na_2^+ . Such an absorption window provides an answer to the long-standing experimental puzzle. The concentration of Na_2^+ in their measurements is estimated to be about 3%, which is consistent with the experimental conditions. The excellent agreement between our theoretical results of ground Na ($Z=11$) and the experimental results demonstrates that both the electron correlations and the relativistic effects are treated adequately on equal footing. Using the bound and continuum state wave functions with sufficient accuracy, the relative bound-bound radiative transition rates, bound-free photoionization cross sections, and electron impact cross sections, which are vitally important in relative fields, can be calculated with adequate preci-

sion. The stringently tested Breit-Pauli R -matrix code should be useful to provide the indispensable J -resolved atomic physical data of intermediate- Z elements such as C, N, O, Ne, Na, Si, S, etc., which play important roles in astrophysics.

ACKNOWLEDGMENTS

We wish to thank Dr. W.H. Zhang for the initial stage of Na₂⁺ calculations. This work was supported by Ministry of

Science and Technology and Ministry of Education of China, the Key grant Project of Chinese Ministry of Education (No. 306020), the National Natural Science Foundation of China (Grant No. 10574162), the National High-Tech ICF Committee in China, and the Yin-He Super-computer Center, Institute of Applied Physics and Mathematics, Beijing, China, National Basic Research Program of China (Grant Nos. 2001CB610508 and 2006CB0L0408); partial computer time supported by IDRIS-CNRS.

-
- [1] U. Fano and J. Cooper, *Rev. Mod. Phys.* **40**, 441 (1968).
 [2] X. L. Liang *et al.*, *Acta Phys. Sin.* **34**, 1479 (1985).
 [3] J. W. Davenport *et al.*, *J. Chem. Phys.* **78**, 1095 (1983).
 [4] S. T. Manson, *Phys. Rev. A* **3**, 1260 (1971).
 [5] H. P. Saha, C. Froese-Fischer, and P. W. Langhoff, *Phys. Rev. A* **38**, 1279 (1988).
 [6] E. M. Isenberg, S. L. Carter, H. P. Kelly, and S. Salomonson, *Phys. Rev. A* **32**, 1472 (1985).
 [7] A. Dasgupta and A. K. Bhatia, *Phys. Rev. A* **31**, 759 (1985).
 [8] J. C. Weisheit, *Phys. Rev. A* **5**, 1621 (1972).
 [9] R. D. Hudson *et al.*, *J. Opt. Soc. Am.* **57**, 651 (1967).
 [10] P. G. Burke *et al.*, *J. Phys. B* **4**, 153 (1971).
 [11] K. A. Berrington *et al.*, *Comput. Phys. Commun.* **8**, 149 (1971).
 [12] K. A. Berrington *et al.*, *Comput. Phys. Commun.* **14**, 346 (1978).
 [13] K. A. Berrington *et al.*, *J. Phys. B* **20**, 6379 (1987).
 [14] L. VoKy, H. E. Saraph, W. Eissner, Z. W. Liu, and H. P. Kelly, *Phys. Rev. A* **46**, 3945 (1992).
 [15] K. A. Berrington and A. E. Kingston, *J. Phys. B* **20**, 6631 (1987).
 [16] K. A. Berrington *et al.*, *Comput. Phys. Commun.* **92**, 290 (1995).
 [17] G. X. Chen, A. K. Pradhan, and W. Eissner, *J. Phys. B* **36**, 453 (2003).
 [18] U. Fano *et al.*, *Phys. Rev. Lett.* **31**, 1573 (1973).
 [19] P. G. Burke *et al.*, *Adv. At. Mol. Phys.* **11**, 143 (1975).
 [20] N. S. Scott and P. G. Burke, *J. Phys. B* **14**, 4299 (1980).
 [21] X. Y. Han *et al.* (unpublished).
 [22] NIST Atomic Spectra Database Levels Form (http://physics.nist.gov/PhysRefData/ASD/levels_form.html).
 [23] U. Fano, *Phys. Rev.* **178**, 131 (1969).
 [24] K. P. Huber and G. Herzberg, *Molecular Spectra and Molecular Structure. IV. Constants of Diatomic Molecules* (Van Nostrand Reinhold Company, New York, 1979).
 [25] D. Dill *et al.*, *J. Chem. Phys.* **61**, 692 (1974).
 [26] X. L. Liang *et al.*, *Chin. Phys. Lett.* **2**, 545 (1985).
 [27] P. H. Zhang and J. M. Li, *Phys. Rev. A* **54**, 665 (1996).
 [28] X. C. Pan *et al.*, *Acta Phys. Sin.* **36**, 426 (1987).
 [29] L. Liu *et al.*, *J. Phys. B* **24**, 1893 (1991).
 [30] J. C. Slater, *J. Chem. Phys.* **43**, S228 (1965).
 [31] U. Fano, *Phys. Rev. A* **2**, 353 (1970).
 [32] C. M. Lee and Jia-Ming Li, *Phys. Rev. A* **6**, 109 (1977).
 [33] C. Jungen and O. Atabek, *J. Chem. Phys.* **66**, 5584 (1977).
 [34] X. M. Tong and J. M. Li, *J. Phys. B* **24**, 1983 (1991).
 [35] W. H. Zhang *et al.* (unpublished).